

Research Paper

Predicting the Solubility of the Anti-Cancer Agent Docetaxel in Small Molecule Excipients using Computational Methods

Loan Huynh,¹ Justin Grant,¹ Jean-Christophe Leroux,² Pascal Delmas,³ and Christine Allen^{1,4}

Received February 5, 2007; accepted July 16, 2007; published online August 18, 2007

Purpose. To develop an *in silico* model that provides an accurate prediction of the relative solubility of the lipophilic anticancer agent docetaxel in various excipients.

Materials and Methods. The *in silico* solubility of docetaxel in the excipients was estimated by means of the solubility (δ) and Flory-Huggins interaction (χ_{FH}) parameters. The δ values of docetaxel and excipients were calculated using semi-empirical methods and molecular dynamics (MD) simulations. Cerius² software and COMPASS force-field were employed for the MD simulations. The χ_{FH} values for the binary mixtures of docetaxel and excipient were also estimated by MD simulations.

Results. The values obtained from the MD simulations for the solubility of docetaxel in the various excipients were in good agreement with the experimentally determined values. The simulated values for solubility of docetaxel in tributyrin, tricaproin and vitamin E were within 2 to 6% of the experimental values. MD simulations predicted docetaxel to be insoluble in β -caryophyllene and this result correlated well with experimental studies.

Conclusions. The MD model proved to be a reliable tool for selecting suitable excipients for the solubilization of docetaxel.

KEY WORDS: docetaxel; excipients; Flory-Huggins interaction parameter; molecular dynamics simulations; solubility parameters.

INTRODUCTION

Drug formulations are employed as a means to improve the solubility, stability, toxicity and/or efficacy of a drug (1–3). The formulations are most often formed from excipients such as phospholipids, medium-chain triglycerides and polymers (3–6). The physico-chemical characteristics of the drug-excipient blend are known to determine the properties and performance of the formulation (7,8). Specifically, the drug loading and retention properties of the formulation are largely influenced by the solubility of the drug in the excipient or miscibility of the drug-excipient blend as well as the presence of specific interactions between the drug and the excipient (9,10).

To date, the development of most drug formulations proceeds largely by trial and error with no clear method of predicting which excipient or material is most appropriate. In this way, the selection of a suitable excipient or material can be a time consuming and expensive endeavour. Computer

simulation of drug-excipient mixtures provides an attractive alternative for predicting the solubility of drugs in excipients.

Recently, atomistic simulations were shown to provide an accurate prediction of the compatibility between polymer-small molecule (11–15) and polymer–polymer blends (16,17). In the area of drug formulation and delivery, computer simulation has mostly been employed to predict the rate of diffusion of a drug in a matrix as a means to elucidate the mechanism of drug release (14,18). For example, Jacobson investigated the diffusion of drugs in a Duro-Tak polymer matrix (i.e. pressure-sensitive adhesive acrylic polymers used in transdermal drug delivery), in the presence and absence of an external force, using molecular dynamics (MD) simulations with the Discover module (InsightII software; 18). The diffusion coefficients that were obtained for various drugs (e.g. nicotine, estradiol, sodium salicylate) in the polymer matrix were related to the polymer-drug interactions and the free volume of the polymer (18). In a few cases, computer simulations have been employed to predict other properties of drug delivery systems (e.g. morphology, stability and interactions) at the molecular and coarse-grain levels (19–22). For example, Poupaert and Couvreur calculated the interaction energy between the anticancer drug doxorubicin and *n*-butyl polycyanoacrylate using molecular simulations (15). From the calculated interaction energy, it was possible to identify the site of interaction for the drug and the functional groups of the polymer that are involved in the interaction (15).

In this study, we report an *in silico* method for predicting the solubility of the anti-cancer agent docetaxel (DTX) in

Electronic supplementary material The online version of this article (doi:10.1007/s11095-007-9412-3) contains supplementary material, which is available to authorized users.

¹ Faculty of Pharmacy, University of Toronto, Toronto, Ontario M5S 3M2, Canada.

² Canada Research Chair in Drug Delivery, Faculty of Pharmacy, University of Montreal, Quebec, H3C 3J7, Canada.

³ Bioxel Pharma Inc., Quebec, G1W 4Y5, Canada.

⁴ To whom correspondence should be addressed. (e-mail: cj.allen@utoronto.ca)

excipients using full atomistic simulation. DTX is a member of the taxoid family and is approved for use in the treatment of prostate, gastric, lung, breast and head and neck cancers (23–30). The primary objective of this research was to evaluate the accuracy and reliability of various *in silico* methods as a means to select suitable excipients for development of an emulsion formulation of DTX. The ability of an excipient to solubilize DTX may be expressed in terms of the Hildebrand solubility parameter (δ_{HIL}) which describes the behavior of apolar and non-interacting liquids (31). However, the presence of hydrogen-bonding interactions can also influence the solubility of compounds (10,32,33). Therefore, in order to more accurately describe the behavior of the mixtures with consideration given to the polar effects and hydrogen-bonding interactions, the Hansen solubility parameter (δ_{HAN}) and Flory-Huggins interaction parameter (χ_{FH}) were calculated (31). Semi-empirical methods and MD simulations were employed to evaluate the solubility parameters (δ) for DTX and excipients (34–36). Furthermore, MD simulations were used to calculate χ_{FH} for drug and excipient pairs. The values obtained for χ_{FH} were used to predict the solubility of DTX in the excipients (36).

MATERIALS AND METHODS

Materials

Anhydrous DTX (99.8%) was obtained from Sai Life Sciences (Hyderabad, India). Tricaprylin (90%), tricaproin ($\geq 99\%$), tributyrin ($\geq 98\%$), vitamin E ($\geq 97\%$), and β -caryophyllene ($\geq 80\%$) and high performance liquid chromatography (HPLC) grade solvents were purchased from Sigma Aldrich (Oakville, ON, Canada) and used as received.

Evaluation of Solubility of DTX in Excipients

The solubility of DTX was evaluated in tricapyrylin, vitamin E, tricaproin, tributyrin, and β -caryophyllene at room temperature using the method established by Higuchi and Connors with slight modification (37–40). A rough estimate of the solubility of DTX in each excipient was first obtained by preparing a series of DTX-excipient mixtures that varied systematically in terms of the initial weight percentage of DTX. Specifically, aliquots of a stock solution of DTX dissolved in ethanol were added to glass vials that were then dried under nitrogen and in a vacuum oven overnight to produce DTX films. The excipients were then added to the DTX films and the mixtures were vortexed and stirred for 8 h at room temperature. DTX and vitamin E were allowed to stir for 24 h due to the viscous nature of these mixtures. Longer stirring times (i.e. 48 h for DTX-vitamin E and 24 h for all other DTX-excipient mixtures) were tried and found to yield comparable values for equilibrium solubility. Aliquots of the DTX-excipient mixtures were transferred to eppendorf tubes and centrifuged for 50 min at 20,000 g (Eppendorf 5804R, Eppendorf Inc., Hamburg, Germany) in order to separate the solution (i.e. supernatant) from the undissolved fraction of DTX (i.e. precipitate). The supernatant was collected and the concentration of dissolved drug was

determined by HPLC analysis. Once an estimate of the solubility of DTX in each excipient had been obtained, the equilibrium solubility was measured by mixing each excipient with excess DTX ($n=5$). The mixtures of excess DTX and excipient were stirred and processed as outlined above.

HPLC Analysis

DTX was extracted from the excipients using a previously reported method with slight modifications (41–43). The mixtures of DTX in excipients were added to an acetonitrile: water: hexane mixture (45:5:50 v/v/v) and processed for HPLC analysis. The extraction efficiency of DTX was found to be $94\pm 4\%$ ($n=6$) from tributyrin, $88\pm 5\%$ ($n=6$) from tricaproin, $95\pm 3\%$ ($n=6$) from tricapyrylin, $95\pm 3\%$ ($n=6$) from vitamin E, and $59\pm 9\%$ ($n=6$) from β -caryophyllene.

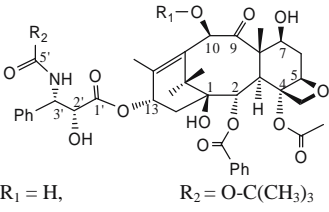
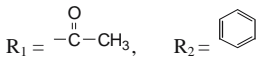
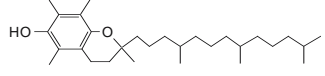
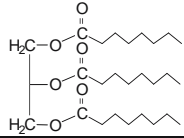
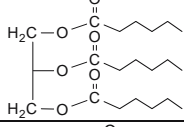
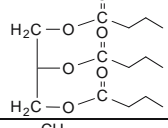
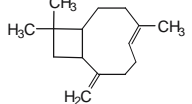
The DTX concentration was measured using an HPLC (Perkin-Elmer series 200 Liquid Chromatograph, Perkin-Elmer Inc., Wellesley, MA) equipped with a Perkin-Elmer 785A UV/VIS detector, Perkin-Elmer Advanced LC sample processor and an XTerra C₁₈ reverse-phase column (particle size, 5 μm) of dimensions 4.6 \times 250 mm (Waters Inc., Milford, MA). The concentration of DTX was detected at a wavelength of 227 nm. For DTX in tricapyrylin, tricaproin, tributyrin or β -caryophyllene, the mobile phase (acetonitrile and water, 53:47 v/v) was eluted isocratically. For DTX in vitamin E, an HPLC gradient elution method was employed. Specifically, a mobile phase of acetonitrile: water (53:47 v/v) was used for the first 15 min to elute DTX followed by a mixture of acetonitrile: water: THF (53:22:25 v/v/v) for 6 min to elute vitamin E. Standard curves were constructed for DTX in each excipient and a linear range was obtained from 5.0 to 120.0 $\mu\text{g/ml}$ DTX for all excipients. The retention time of DTX was 8 min at a flow rate of 1.0 ml/min.

Computational Methodology

Calculation of Solubility Parameters using Group Contribution Methods and C²-Synthia Module

In this study, the δ_{HIL} and δ_{HAN} values were used to quickly gain an estimate of the solubility of DTX in excipients based on the chemical structures of the molecules (Table I). The semi-empirical methods, including group contribution methods (GCM; 44) and C²-Synthia module from Cerius² software (36,45), were used to calculate the δ_{HIL} and δ_{HAN} by applying the Fedors (34) and Hoftyzer-Van Krevelen (34,35) approaches, respectively. The δ_{HIL} is defined as the square root of the cohesive energy density (CED), which is the heat or energy of vaporization of a material per unit volume in the amorphous state at room temperature (44). The Fedors method for determination of the δ_{HIL} ($\delta_{\text{HIL-GCM}}$ and $\delta_{\text{HIL-Syn}}$) involves summation of the cohesive energy (E_{coh}) and volume (V) contributions from the individual functional groups within the molecule (34,44). In comparison, Hoftyzer-Van Krevelen's method for determination of the δ_{HAN} ($\delta_{\text{HAN-GCM}}$ and $\delta_{\text{HAN-Syn}}$) takes into account the different types of intermolecular forces (34,35). Therefore, the δ_{HAN} (Eq. 1) is obtained from the partial solubility parameters (i.e. δ_{d} , δ_{p} and δ_{h} , Eqs. 2, 3, 4)

Table I. Chemical Structures and Properties of Drugs and Excipients

Drugs/Excipients	Chemical structure	Molecular Weight (g/mol)	V_{Molar}^a (cm ³ /mol)	Density ^a (g/cm ³)	MP/BP (°C)	Water solubility [µg/mL]	Appearance
Docetaxel		807.9	664.4	1.216	MP: 232 ^b	5.0 – 6.0 (78)	White crystalline powder
Paclitaxel		853.9	688.3	1.235	MP: 223 (70)	0.30 (78)	White crystalline powder
Vitamin E (d-α-Tocopherol)		430.7	453.4	0.950	MP: 2.5 - 3.5 BP: 200 - 220 ^b	insoluble	Very faint yellow, clear viscous liquid
Tricaprylin (C8:0)		470.7	492.4	0.953	MP: 9 - 10 ^b BP: 233 ^b	insoluble	Colourless, clear liquid
Tricaproin (C6:0)		386.5	394.4	0.980	NA	0.45 (5)	Colourless, clear liquid
Tributyrin (C4:0)		302.4	293.0	1.032	BP: 129 - 131 ^b	133.4 (5)	Colourless, clear liquid
β-Caryophyllene		204.3	226.5	0.902	BP: 262 - 264 ^b	insoluble	Colourless, clear liquid

(a) Molar volumes (V_{Molar}) of excipients were calculated from the experimental density and molecular weight of the excipients. V_{Molar} and density of drugs were obtained by using C²-Synthia module. (b) MP/BP: melting point/boiling point were obtained from the material safety data sheet.

which are calculated from values assigned to specific functional groups for dispersion (F_d), dipole-dipole (F_{pi}), hydrogen-bonding (F_{hi}) interactions as well as volume (V ; 45).

$$\delta_{\text{HAN}} = \sqrt{(\delta_d^2 + \delta_p^2 + \delta_h^2)} \quad (1)$$

$$\delta_d = \frac{\sum F_d}{V} \quad (2)$$

$$\delta_p = \frac{\sqrt{\sum F_{pi}^2}}{V} \quad (3)$$

$$\delta_h = \frac{\sqrt{\sum E_{hi}}}{V} \quad (4)$$

Theoretically, the smaller the difference between the values for δ of the solute and solvent, the greater the solubility of the solute in the solvent (31,44,46,47). It has been reported that values for $\Delta\delta$ of less than 7.5 (J/cm³)^{1/2} for a solute-solvent pair indicate that the solute has a good solubility in the solvent (31).

Calculation of Solubility Parameters using MD Simulation

MD is a force-field based simulation method that is used to calculate the behavior of molecules in a time dependent manner (48,49). MD takes into account the molecular motions (e.g. simple vibrations, bond stretching and angle bending) that occur within a system (48). MD simulations were used to calculate the δ_{HIL} values ($\delta_{\text{HIL-MD}}$) of DTX and excipients as well as the χ_{FH} for the DTX-excipient pairs. The Ewald method with application of the COMPASS (Condensed-phase Optimized Molecular Potentials for Atomistic Simulation Studies; 50) force-field was used to calculate the Coulombic and attractive van der Waals (vdW) interac-

tions (51). For the COMPASS force-field, the total energy (E_{total}) of a system is represented by the sum of the valence interactions (E_{valence}), non-bonding interactions ($E_{\text{non_bond}}$) and the cross-coupling term ($E_{\text{crossterm}}$; 50,51):

$$E_{\text{total}} = E_{\text{valence}} + E_{\text{crossterm}} + E_{\text{non_bond}} \quad (5)$$

The E_{valence} consists of bond stretching (E_{bond}), angle energy (E_{angle}), torsion angle rotations (E_{torsion}), out-of-plane (E_{oop}) and Urey-Bradley interactions (E_{UB} ; 50):

$$E_{\text{valence}} = E_{\text{bond}} + E_{\text{angle}} + E_{\text{torsion}} + E_{\text{oop}} + E_{\text{UB}} \quad (6)$$

The $E_{\text{crossterm}}$ includes the following interaction energies: the stretch-stretch ($E_{\text{bond-bond}}$), stretch-bend ($E_{\text{bond-angle}}$), bend-bend ($E_{\text{angle-angle}}$), stretch-torsion ($E_{\text{central-bond-torsion}}$ and $E_{\text{terminal-bond-torsion}}$), bend-torsion ($E_{\text{angle-torsion}}$) and bend-bend-torsion ($E_{\text{angle-angle-torsion}}$; 50,52):

$$\begin{aligned} E_{\text{crossterm}} = & E_{\text{bond-bond}} + E_{\text{bond-angle}} + E_{\text{angle-angle}} \\ & + E_{\text{central-bond-torsion}} + E_{\text{terminal-bond-torsion}} \\ & + E_{\text{angle-torsion}} + E_{\text{angle-angle-torsion}} \end{aligned} \quad (7)$$

The interaction energy between non-bond atoms is comprised of the vdW interaction energy (E_{vdW}) and the electrostatic interaction energy (E_{Coulomb}), which is calculated by a Coulombic function based on the partial charges of the atoms in the system (51):

$$E_{\text{non_bond}} = E_{\text{vdW}} + E_{\text{Coulomb}} \quad (8)$$

The difference in the E_{total} of the molecules in the vacuum state (E_{vac}) and the amorphous state (E_{bulk}) can be employed to calculate the δ_{HIL} which may be defined by the following equation (16):

$$\delta_{\text{HIL}} = \sqrt{\frac{E_{\text{coh}}}{V}} = \sqrt{\frac{(E_{\text{vac}} - E_{\text{bulk}})C}{V}} = \sqrt{\text{CED}} \quad (9)$$

where V is the volume of the periodic cell in cubic angstroms. The units for E_{coh} obtained from the MD simulation are expressed in (kcal/(molÅ³)), which are then converted to J/cm³ using the converting factor C that is calculated as follows:

$$\begin{aligned} C &= \frac{\text{kcal}}{\text{mol Å}^3} = \frac{4184 \text{ J}}{\text{N}_A 1 \times 10^{-24} \text{ cm}^3} \\ &= \frac{4184 \text{ J}}{(6.022 \times 10^{23})(1 \times 10^{-24} \text{ cm}^3)} = 6947.86 \frac{\text{J}}{\text{cm}^3} \end{aligned}$$

Calculation of Flory-Huggins Interaction Parameters and Prediction of Solubility using MD Simulation

Theoretically, at a specific temperature, the solubilization of a solute in a solvent (i.e. one phase solution) is attributed to favourable entropic (i.e. positive) and/or enthalpic (i.e. negative) contributions that are reflected by either a small positive or a negative energy of mixing (ΔE_{mix}). ΔE_{mix} for DTX-excipient mixtures was calculated from the

CED of the pure DTX ($[E_{\text{coh}}/V]_{\text{DTX}}$), pure excipient ($[E_{\text{coh}}/V]_{\text{EXC}}$) and DTX-excipient mixtures ($[E_{\text{coh}}/V]_{\text{DTX-EXC}}$) using Eq. 10 (16).

$$\begin{aligned} \Delta E_{\text{mix}} = & \phi_{\text{DTX}} \left(\frac{E_{\text{coh}}}{V} \right)_{\text{DTX}} + \phi_{\text{EXC}} \left(\frac{E_{\text{coh}}}{V} \right)_{\text{EXC}} \\ & - \left(\frac{E_{\text{coh}}}{V} \right)_{\text{DTX-EXC}} \end{aligned} \quad (10)$$

where ϕ_{DTX} and ϕ_{EXC} are the volume fractions of DTX and excipient in the binary mixed system, respectively. E_{coh} is the cohesive energy and V is the total volume of the system. The volume fraction (ϕ_i) can be defined as $\phi_i = (n_i V_i / V)$, where n_i is the number of moles and V_i is the volume of compound i (53).

In this study, χ_{FH} values were calculated using Eq. 11 (54,55).

$$\chi_{\text{FH}} = \frac{V_{\text{ref}} \Delta E_{\text{mix}}}{RT} \quad (11)$$

where V_{ref} is equal to the molar volume of the excipient (i.e. smaller molecule in the binary mixtures) that is obtained from the experimental density and molecular weight of the excipient. χ_{FH} was originally introduced, in Flory-Huggins (FH) theory, to describe the interactions in polymer-solvent systems (56). FH theory is a lattice-based model that was put forth to characterize the thermodynamic behavior of apolar and dilute polymer solutions (53,56). This theory was developed with the assumptions that the configuration of molecules within the system is completely random and that no specific interactions are created or destroyed upon mixing of the two components (56). The MD simulations performed in these studies are based on modified-FH theory that takes into account specific intermolecular interactions present between the two components within the mixture (55). This modified-FH theory also allows for evaluation of the concentration dependence of χ_{FH} (55).

The relationship between χ_{FH} and the Gibbs energy of mixing (ΔG_{mix}) is as follows (53,57):

$$\Delta G_{\text{mix}} = RT[n_1 \ln \phi_1 + n_2 \ln \phi_2 + n_1 \phi_2 \chi_{\text{FH}}] \quad (12)$$

where n_i and ϕ_i are the number of moles and volume fraction of components 1 and 2, respectively. The first two terms are said to account for combinatorial entropy contributions while the third term is an enthalpic contribution (57). For the solution to be miscible ΔG_{mix} must be negative, thus the enthalpic term must have a negative value or a positive value that is less in magnitude than that of the entropic contribution (57). Therefore, as χ_{FH} approaches zero or negative values, spontaneous mixing of the two component system is favoured.

Theoretically, as outlined in the Appendix A (53,56,58), phase separation of a polymer-solvent mixture begins to occur at the ‘‘critical’’ point when χ_{FH} is equal to 0.5 (i.e. $\chi_{\text{FH,crit}}$). The ‘‘critical’’ values for χ_{FH} can be expressed in terms of volume fraction as shown in Eq. 13 (53,56,58).

$$\chi_{\text{FH,crit}} = 1/2(1 - \phi_2)^{-2} \quad (13)$$

Indeed, χ_{FH} values of less than 0.5 have been obtained experimentally for a range of miscible polymer-solvent

Table II. The Properties of the Pure Component and the Binary Mixed Systems of Docetaxel (DTX) and Excipients in the Amorphous Cells

Volume Fraction of DTX (ϕ_{DTX})	Number of DTX : Tributyrin molecules	Number of DTX : Tricaproin molecules	Number of DTX : Tricaprylin molecules	Number of DTX : Vitamin E molecules	Number of DTX : β -Caryophyllene molecules
1.000	40: 0 (1.216)				
0.000	0:94 (1.032)	0:68 (0.980)	0:55 (0.953)	0:58 (0.950)	0:114 (0.902)
0.025	1:88 (1.034)	1:66 (0.984)	1:53 (0.961)	1:57 (0.955)	1:114 (0.905)
0.050	2:86 (1.036)	2:64 (0.987)	2:51 (0.966)	2:56 (0.959)	2:111 (0.908)
0.075	3:84 (1.038)	3:62 (0.991)	3:50 (0.971)	3:54 (0.964)	3:109 (0.910)
0.100	4:82 (1.041)	4:61 (0.995)	4:49 (0.976)	4:53 (0.969)	4:106 (0.913)

Values in parentheses are the density (g/cm^3) of the amorphous cells.

solutions (59,60). In this study, the χ_{FH} values obtained from MD simulations of each DTX-excipient mixture were plotted as a function of ϕ_{DTX} . The values for ϕ_{DTX} at $\chi_{\text{FH}}=0.50$ were then taken to be the predicted maximum solubility of DTX in each excipient.

Simulation Methodology

MD simulations were performed using Cerius² (C²) software (version 4.6) from Accelrys Inc. (San Diego, CA.) on a Silicon Graphics OCTANE workstation (IRIX 6.5 operating system) that connects to an Onyx3800 supercomputer (44 MIPS processors) at the Molecular Design and Information Technology Center (University of Toronto, Ontario). One processor was used per simulation of drug, excipient or mixtures of drug and excipient with an average processing time of approximately four months. The pure drug, excipients and their mixtures were built in periodic cells using the C²-Amorphous module. The density of the single-components and the mixed systems were defined according to the experimental density of excipients and the calculated density of DTX (i.e. obtained from C²-Synthia module) in order to mimic the experimental conditions. MD simulations were performed on the constructed periodic systems using C²-Dynamics module. The periodic cells of the pure component or binary mixtures contained approximately 5,000 atoms in a cell of $35\text{\AA} \times 35\text{\AA} \times 35\text{\AA}$ (as detailed further in Table II). The non-bond cutoff for the vdW terms was applied with a cutoff distance of 8.5\AA (50,51). This optimal cutoff distance was less than half of the dimension of the cell.

The simulation methodology for the pure and binary mixed systems is outlined in Fig. 1. All of the periodic cells were constructed and analyzed to ensure a homogenous distribution of molecules in the periodic system. In addition, sufficient interaction between the two components (i.e. no “empty holes”) within the initial configuration of the binary system was also required for MD simulation (16). The optimal systems were minimized using the “Smart Minimizer” algorithms for 5,000 steps or until the maximum derivative (i.e. root-mean-square of the potential energy gradient) was less than $0.001\text{ kcal}/\text{mol}/\text{\AA}$ (61). Following the energy minimization step, Nosé-Hoover constant-temperature, constant-volume ensemble (NVT) was applied to the system at 298 K (62,63). The time required to reach the equilibrium state depended on the size of the system and the molecular structure of the components (48).

The general methodology for MD simulations includes two stages: equilibration and production (or data-collection; 36). Initially, the velocities are randomly assigned to atoms in the model according to the Maxwell-Boltzmann distribution. A time step of 1 fs was used with a minimum runtime of 100 ps for the equilibration stage. For the production stage, the MD simulation time was 800 ps or until equilibrium was reached (i.e. maximum 2,200 ps). The configurations from MD simulations were saved every 1 ps to the trajectory file. Finally, the CED were evaluated over the last 50 ps of the MD simulations (51). In this study, ϕ_{DTX} in the various excipients ranged from 0.025 to 0.100. A typical example of the initial configuration of a periodic cell containing two DTX and 86 tributyrin molecules (i.e. $\phi_{\text{DTX}}=0.050$) is shown in Fig. 2.

RESULTS AND DISCUSSION

Experimental Solubility

The excipients selected for this research include vitamin E (i.e. d- α -tocopherol), tributyrin, tricaproin, tricaprylin and β -caryophyllene which are all generally recognized as safe and/or listed by the Food and Drug Administration for use as pharmaceutical or food additives (Table I; 64–69). As listed in Table III, the experimental solubility of DTX in the various excipients ranged from 0.4 to 108 mg/ml with the

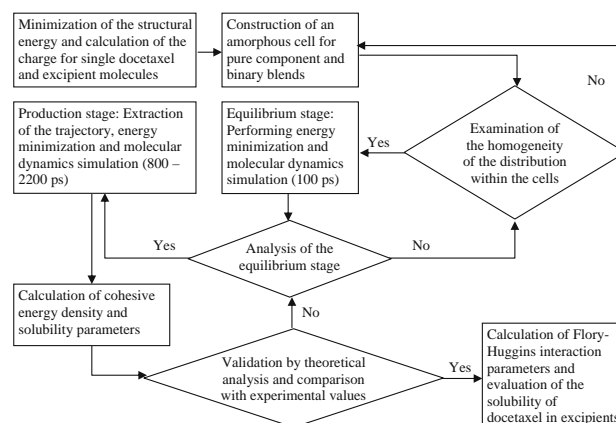


Fig. 1. Flowchart of approach taken for molecular dynamics simulations of the pure and binary mixed systems of docetaxel and excipient.

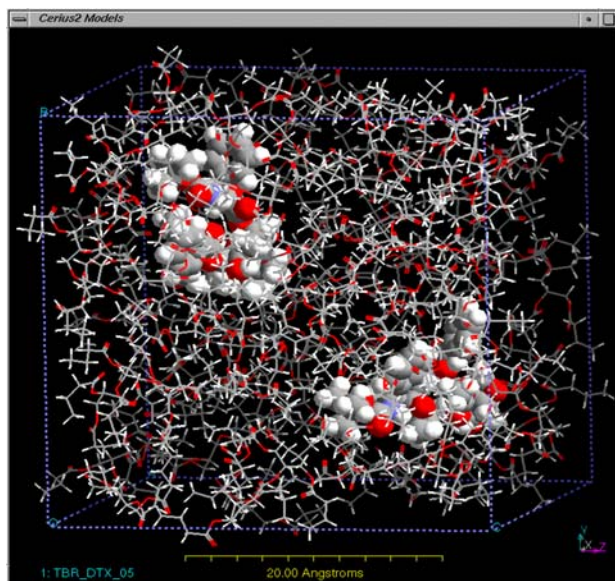


Fig. 2. An amorphous cell containing 2 docetaxel and 86 tributyrin molecules. Tributyrin and docetaxel are shown by stick and space-filling representations, respectively.

solubility being highest in tributyrin. The solubility of DTX in the saturated, medium-chain triglycerides [i.e. tributyrin (C4:0), tricaproin (C6:0) and tricapyrylin (C8:0)] increased with a decrease in the hydrocarbon chain length. These results are in agreement with a study by Kan *et al.* which found that the solubility of paclitaxel (PTX) in various triglycerides [i.e. tributyrin, tricaproin, tricapyrylin and triacetin (C2:0)] increased as the length of the hydrocarbon chain of the triglyceride decreased (5). PTX is a clinically relevant analog of DTX and their structures vary in terms of the functional groups present at the C-10 and C-5' positions, as shown in Table I. It has been reported that in the presence of triglycerides, the intra- and intermolecular hydrogen-bonding between PTX molecules is replaced by hydrogen-bonding interactions between the drug and the triglyceride molecules (2,70,71). The solubility of PTX or DTX in triglycerides may be related to their potential to engage in hydrogen-bonding interactions with the carbonyl functional group of the triglyceride. Indeed, the number of moles of the carbonyl functional groups available to form hydrogen bonds with DTX was highest for tributyrin (1.13×10^{-3} mol) in comparison to tricaproin (0.85×10^{-3} mol) and tricapyrylin (0.68×10^{-3} mol), per ml of triglyceride.

The hydrogen-bonding interactions between DTX and these relatively hydrophobic excipients are intermolecular interactions that only act to enhance the solubility of the drug. It is postulated that the drug's solubility in these excipients is mostly attributed to dispersion and other vdW forces that are known to exist between hydrophobic drugs and hydrophobic excipients (72,73).

In Silico Solubility Parameters for DTX and Excipients

The solubility parameters of DTX (δ_{DTX}) and excipients (δ_{EXC}) were determined by *in silico* methods as listed in Table IV. For each DTX-excipient pair, we calculated the difference between δ_{DTX} and δ_{EXC} values ($\Delta\delta$) obtained from GCM ($\Delta\delta_{\text{HIL-GCM}}$, $\Delta\delta_{\text{HAN-GCM}}$), C²-Synthia module ($\Delta\delta_{\text{HIL-Syn}}$, $\Delta\delta_{\text{HAN-Syn}}$) and MD ($\Delta\delta_{\text{HIL-MD}}$) in order to screen for excipients that are most suitable for solubilization of DTX (Table V). As discussed previously, a lower value for $\Delta\delta$ for a specific DTX-excipient pair should result in a higher solubility for DTX in that excipient. However, if one compound contains functional groups that are strongly polar and/or have hydrogen donor/acceptor capability while the other compound does not, the mixture may be immiscible even if the δ values of the two compounds are the same (44). This is due to the fact that the δ_{HIL} was initially proposed for only apolar, non-associating liquid (i.e. solvent) systems (44). The ability of the computational methods to enable an accurate selection of the optimal excipient for DTX was verified by comparison with the experimentally determined values for solubility. According to values obtained for $\Delta\delta$ from the semi-empirical methods, the estimated solubility of DTX in the excipients decreased in the following order:

- From $\Delta\delta_{\text{HAN-GCM}}$ values:
- Vitamin E > Tributyrin > Tricaproin > β Caryophyllene \approx Tricapyrylin
- From $\Delta\delta_{\text{HIL-GCM}}$ and $\Delta\delta_{\text{HAN-Syn}}$ values:
- Vitamin E > Tributyrin > Tricaproin > Tricapyrylin > β Caryophyllene
- From $\Delta\delta_{\text{HIL-Syn}}$ values:
- Tributyrin > Tricaproin > Vitamin E \approx Tricapyrylin > β Caryophyllene

Calculations using the GCM and C²-Synthia module accurately predicted the relative degree of solubility of DTX in the triglycerides (i.e. tributyrin, tricaproin, tricapyrylin) as the ranking was in agreement with the experimental results.

Table III. Experimentally Determined and MD Simulated Values for the Solubility of Docetaxel in the Various Excipients at Room Temperature

Excipients	Experimental Solubility (mg/ml) ^a	Simulated Solubility (mg/ml) ^b
Tributyrin	108±1.8 (colourless, clear liquid)	114.4 (0.086)
Tricaproin	85.7±2.0 (colourless, clear liquid)	88.7 (0.068)
Vitamin E	75.0±1.8 (very faintly yellow, clear viscous liquid)	76.2 (0.059)
Tricapyrylin	55.6±2.2 (colourless, clear liquid)	65.3 (0.051)
β -Caryophyllene	0.43±0.09 (colourless, clear liquid)	< 31.2 (<0.025)

^a Values are the mean of five measurements; the physical appearance of the docetaxel-excipient solutions are described in parentheses.

^b The simulated solubility was taken to be the volume fraction of docetaxel (values in parentheses) that corresponded to a value for the Flory-Huggins interaction parameter of 0.5 (Fig. 4).

Table IV. Hildebrand and Hansen Solubility Parameters of Docetaxel and Excipients Calculated Using Group Contribution Methods, C²-Synthia Module and Molecular Dynamics Simulations at 298 K

Compounds	$\delta_{\text{HAN-GCM}}^{a, b}$	$\delta_{\text{HIL-GCM}}^c$	$\delta_{\text{HAN-Syn}}^a$	$\delta_{\text{HIL-Syn}}^c$	$\delta_{\text{HIL-MD}}^c$
Docetaxel	27.14 (21.91, 3.51, 15.63)	28.28	23.88	24.26	20.17
Tributyryn	18.90 (16.54, 3.01, 8.62)	19.84	17.84	20.53	18.89
Tricaproin	18.33 (16.60, 2.24, 7.44)	19.27	17.57	19.77	18.13
Vitamin E	19.50 (17.91, 1.59, 7.55)	20.08	19.29	19.30	17.81
Tricaprylin	18.00 (16.64, 1.78, 6.65)	18.93	17.41	19.31	17.76
β -Caryophyllene	18.03 (18.03, 0.00, 0.00)	18.37	17.03	17.87	16.86

The values for δ are expressed in $(\text{J}/\text{cm}^3)^{1/2}$.

^aHansen solubility parameters obtained using group contribution methods ($\delta_{\text{HAN-GCM}}$) and C²-Synthia module ($\delta_{\text{HAN-Syn}}$)

^bValues in parentheses are Hansen partial solubility parameters including δ_d , δ_p and δ_h , respectively.

^cHildebrand solubility parameters obtained using group contribution methods ($\delta_{\text{HIL-GCM}}$), C²-Synthia module ($\delta_{\text{HIL-Syn}}$), and molecular dynamics simulation ($\delta_{\text{HIL-MD}}$).

Furthermore, the relative degree of solubility predicted from the $\Delta\delta_{\text{HIL-Syn}}$ was similar to the experimental results with the exception that DTX was predicted to be equally soluble in vitamin E and tricapyrylin. The predicted solubility, according to the values of $\Delta\delta_{\text{HAN-GCM}}$, $\Delta\delta_{\text{HIL-GCM}}$ and $\Delta\delta_{\text{HAN-Syn}}$ for the DTX-vitamin E and DTX- β -caryophyllene pairs, disagreed with the experimental results. In contrast, the values obtained for $\Delta\delta_{\text{HIL-MD}}$ correctly predicted the solubility of DTX in all of the excipients investigated. From the MD results, the solubility of DTX in the various excipients was predicted to decrease in the following order:

Tributyryn>Tricaproin>Vitamin E>Tricaprylin> β -Caryophyllene

The δ_{DTX} values calculated by GCM method ($\delta_{\text{HIL-GCM}}$, $\delta_{\text{HAN-GCM}}$) were significantly larger than the values obtained from C²-Synthia module ($\delta_{\text{HIL-Syn}}$, $\delta_{\text{HAN-Syn}}$) and MD ($\delta_{\text{HIL-MD}}$). Hence, for each of the DTX-excipient pairs investigated, large $\Delta\delta_{\text{HIL-GCM}}$ and $\Delta\delta_{\text{HAN-GCM}}$ values ($>7.6 (\text{J}/\text{cm}^3)^{1/2}$) were obtained (Table V). Therefore, the GCM method was considered less accurate for calculating δ values for large and bulky molecules such as DTX. Nevertheless, the $\delta_{\text{HAN-GCM}}$ values provide details of the interactions that contribute to the total solubility parameter. Given that β -caryophyllene is an apolar solvent, the contributions of polar groups (δ_p) and hydrogen-bonding (δ_h) interactions to the $\delta_{\text{HAN-GCM}}$ value for β -caryophyllene were zero which explains the poor experimental solubility of DTX in β -caryophyllene (Tables III and IV). When considering only the δ_h value, which represents the hydrogen-bonding donor/acceptor

capability of the excipients, tributyrin had the highest δ_h value [$8.6 (\text{J}/\text{cm}^3)^{1/2}$] followed by tricaproin [$7.4 (\text{J}/\text{cm}^3)^{1/2}$] and then tricapyrylin [$6.6 (\text{J}/\text{cm}^3)^{1/2}$]. The δ_h value for vitamin E [$7.6 (\text{J}/\text{cm}^3)^{1/2}$] was slightly larger than tricaproin indicating that vitamin E has the ability to form hydrogen-bonding interactions with DTX. The hydroxyl group within the chemical structure for vitamin E may act as a hydrogen acceptor and donor. Thus, as mentioned previously, the solubility of DTX in the various excipients may be related to the extent of hydrogen-bonding between the drug and excipient. Similar observations were made in studies evaluating the solubility of ibuprofen in various excipients (i.e. poloxamer 188, maltose, sorbitol) in solid dispersion formulations (74).

In excipients that DTX was found experimentally to have good solubility (Table III; i.e. the solubility of DTX in excipient was greater than 50 mg/ml), $\Delta\delta$ values of 3.7–6.5 $(\text{J}/\text{cm}^3)^{1/2}$ and 1.3–2.4 $(\text{J}/\text{cm}^3)^{1/2}$ were obtained from the C²-Synthia module and MD simulations, respectively. For DTX in β -caryophyllene, values of 6.9 $(\text{J}/\text{cm}^3)^{1/2}$ and 6.4 $(\text{J}/\text{cm}^3)^{1/2}$ were obtained for $\Delta\delta_{\text{HAN-Syn}}$ and $\Delta\delta_{\text{HIL-Syn}}$, respectively; whereas, a $\Delta\delta_{\text{HIL-MD}}$ value of 3.3 $(\text{J}/\text{cm}^3)^{1/2}$ was obtained from MD simulations. The values for $\Delta\delta$ obtained from C²-Synthia and MD models were relatively low (i.e. less than 7.5 $(\text{J}/\text{cm}^3)^{1/2}$ for the β -caryophyllene and DTX pair). Yet, from consideration of the relative ranking of the excipients and the chemical structure of β -caryophyllene, it may be deduced that the solubility of DTX in β -caryophyllene is poor. In comparison, DTX and the other excipients investigated can interact as they possess polar and hydrogen-bonding groups. These observations were further confirmed from the values for the Hansen partial solubility

Table V. The Difference Between the Solubility Parameters of Docetaxel and Excipients

Docetaxel/excipient	$\Delta\delta_{\text{HAN-GCM}}^a$	$\Delta\delta_{\text{HIL-GCM}}^b$	$\Delta\delta_{\text{HAN-Syn}}^a$	$\Delta\delta_{\text{HIL-Syn}}^b$	$\Delta\delta_{\text{HIL-MD}}^b$
Docetaxel/Tributyryn	8.24	8.44	6.04	3.73	1.28
Docetaxel/Tricaproin	8.81	9.01	6.31	4.49	2.04
Docetaxel/Vitamin E	7.64	8.20	4.59	4.96	2.36
Docetaxel/Tricaprylin	9.14	9.35	6.47	4.95	2.41
Docetaxel/ β -Caryophyllene	9.11	9.91	6.85	6.39	3.31

The values for $\Delta\delta$ are expressed in $(\text{J}/\text{cm}^3)^{1/2}$.

^aCalculated values using Hansen solubility parameters obtained from group contribution methods ($\Delta\delta_{\text{HAN-GCM}}$) and C²-Synthia module ($\Delta\delta_{\text{HAN-Syn}}$)

^bCalculated values using Hildebrand solubility parameters obtained from group contribution methods ($\Delta\delta_{\text{HIL-GCM}}$), C²-Synthia module ($\Delta\delta_{\text{HIL-Syn}}$) and molecular dynamics simulation ($\Delta\delta_{\text{HIL-MD}}$)

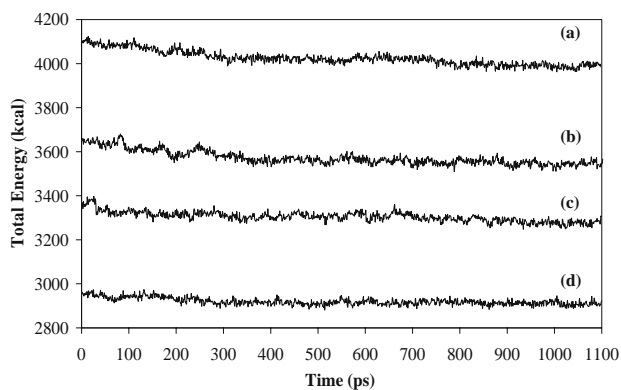


Fig. 3. Nosé-Hoover constant-temperature, constant-volume ensemble equilibrium of docetaxel and (a) tributyrin, (b) tricaproin, (c) tricaprylin and (d) vitamin E pairs at volume fractions of docetaxel of 0.025 for the last 1,100 ps of the simulation.

parameters for polar and hydrogen-bonding contributions (i.e. δ_p and δ_h) as discussed above.

From the results, the MD method was identified as the most reliable and accurate for predicting δ values for the excipients. Also, these results suggest that the COMPASS force-field is suitable for predicting the solubility of DTX in excipients. The MD method accounts for the interactions between atoms (i.e. hydrogen-bonding) within a periodic boundary condition and the many conformations of the compounds (36,48). In contrast, GCM and the C²-Synthia module only consider the contributions from the functional groups of a single molecule (i.e. drug and excipients; 35). The advantages of GCM and C²-Synthia module are that they allow for a fast and straightforward prediction of the δ values.

Evaluation of the Degree of Interaction within the Binary Mixed Systems

The plot of total energy as a function of time for the last 1,100 ps demonstrated that the equilibrium stage was obtained for binary mixtures of DTX and excipients at $\phi_{\text{DTX}}=0.025$ (Fig. 3) (36). No significant changes in the calculated cohesive energy of the binary mixed systems were observed over the last 200 ps of the simulation. Hence, the calculated interaction parameters χ_{FH} were considered as equilibrium values at 25°C.

The results from the MD simulations demonstrated that the χ_{FH} values for mixtures of DTX and excipient increased as a function of ϕ_{DTX} in the binary system (i.e. interactions between DTX and excipients decreased with increasing ϕ_{DTX}). Consistent with the calculated $\delta_{\text{HIL-MD}}$ values and the experimental results, stronger interactions (i.e. smaller χ_{FH} values) were predicted for the DTX-tributyryn pair in comparison to DTX in the other excipients at the same ϕ_{DTX} (Fig. 4). For ϕ_{DTX} ranging from 0.050 to 0.100, the values obtained for χ_{FH} can be related to the ability of the excipient to engage in hydrogen-bonding interactions with DTX. Specifically, similar χ_{FH} values were obtained for DTX in vitamin E ($\delta_h=7.55$) and tricaproin ($\delta_h=7.44$) at ϕ_{DTX} of 0.050; whereas, a lower χ_{FH} values was obtained for DTX in tributyrin ($\delta_h=8.62$) in comparison to DTX in tricaproin, vitamin E or tricaprylin ($\delta_h=6.65$) as shown in Fig. 4 and Table IV.

For DTX and β -caryophyllene mixtures, the calculated χ_{FH} values obtained from the MD simulations were greater than 0.50 for all ϕ_{DTX} (0.025–0.100) indicating complete insolubility for DTX in these mixtures. These results were further supported by the poor solubility of DTX in β -caryophyllene (0.4 mg/ml) that was observed experimentally (Table III). Yet, a ϕ_{DTX} of 0.025 corresponds to a concentration of approximately 31 mg/ml of DTX in β -caryophyllene. In order to calculate the interaction parameter for DTX and β -caryophyllene at lower ϕ_{DTX} (e.g. $\phi_{\text{DTX}}=0.010$ or 12 mg/ml), a periodic cell containing one DTX and 290 β -caryophyllene molecules (e.g. 11,421 atoms) is required for MD simulation. However, MD simulation on a large periodic system (i.e. greater than 10,000 atoms) is impractical as it requires very long simulation times to reach the equilibrium stage. Therefore, simulations at low ϕ_{DTX} in β -caryophyllene were not performed.

In this study, the values for ϕ_{DTX} at $\chi_{\text{FH}}=0.50$ obtained from Fig. 4 were taken to be the maximum solubility of DTX in each excipient (Table III). The values obtained for solubility via MD simulations for DTX in tributyrin, tricaproin or vitamin E were considered accurate in comparison to the experimental results as the percent deviation was between 2 and 6%. However, the simulated solubility of DTX in tricaprylin (65 mg/ml) was approximately 15% above the experimental value (56 mg/ml). The differences between the experimental and simulated solubility values may be attributed to several factors. Firstly, the value for the molar volume of DTX employed in the simulations was obtained using the C²-Synthia module and so considered to be equivalent to the molar volume in vacuo. Thus, the change in volume associated with mixing DTX and excipient was considered to be negligible. However, this likely only has a slight affect on the accuracy of the results since ϕ_{DTX} in the binary mixtures is low. Specifically, the density of the amorphous cell for the binary mixtures of DTX and tributyrin ranged from 0.2 to 0.9% greater than the experimental density of pure tributyrin, whereas; the density for the binary mixtures of DTX and tricaprylin varied from 0.8 to 2.4% greater than pure tricaprylin. It should also be noted that the CED as well as the $\delta_{\text{HIL-MD}}$

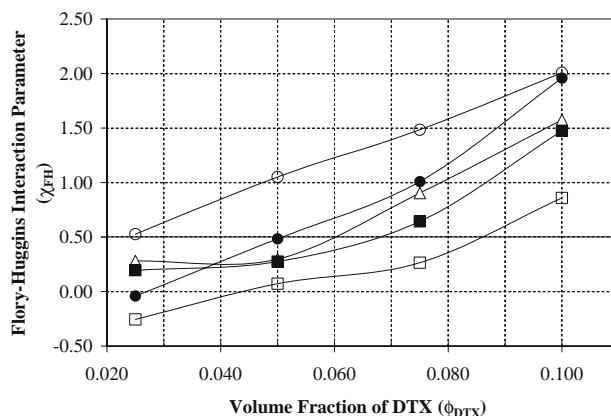


Fig. 4. Flory-Huggins interaction parameter for the binary mixtures of docetaxel and tricaproin (filled circles), tricaproin (filled squares), tributyrin (open squares), vitamin E (open triangles), and β -caryophyllene (open circles) as a function of volume fraction of docetaxel.

were proportional to the volume of the amorphous cell as described in Eq. 9. Secondly, in theory, a homogeneous (i.e. one phase) solution of a two-component system is said to correspond to a value of less than 0.5 for χ_{FH} (53,56,58,75). Yet, the assumption was made that the ϕ_{DTX} at $\chi_{FH}=0.50$ could be converted to the maximum solubility for the compound in the excipient. In this way, the simulated values for solubility are expected to slightly overestimate the actual solubility of the drug in each excipient. Thirdly, as mentioned in the methods section, the MD simulations are based on a modified FH theory. This modified FH theory may overestimate the attractive intermolecular interactions that are present between DTX and the excipients. Thus, the simulated values for χ_{FH} are underestimated which results in an overestimate of the solubility of DTX in the excipients.

The experimental values obtained for the solubility of DTX in the various excipients were used to calculate the “critical” values for χ_{FH} (i.e. when phase separation begins to occur) using Eq. 13 (53,56,58). The values for $\chi_{FH,crit}$ were found to be 0.54, 0.56, 0.57 and 0.59 for DTX in tricaprolylin, vitamin E, tricaproin and tributyrin, respectively. These values are close to but slightly greater than the expected $\chi_{FH,crit}$ value of 0.5. This finding is in agreement with other studies that have shown experimentally that the value of $\chi_{FH,crit}$ can vary depending on the nature and properties of the binary mixture (53,57,60,75–77).

Overall, a good agreement was obtained between the experimental and simulated values for the solubility of DTX in the excipients. However, limitations of this MD simulation method were observed including the inability to estimate the solubility of the drug in poor excipients (i.e. β -caryophyllene). In addition, the discrepancy between the experimental and simulated values for solubility suggests that this method may be most reliably employed for relative ranking of excipients rather than determination of the absolute value of the solubility of a drug in a particular excipient.

CONCLUSIONS

Our computational model accurately predicted the relative solubility of DTX in the various excipients, as the computational results were in agreement with values obtained experimentally. Overall, of the excipients evaluated tributyrin was found to be the most favourable for solubilization of DTX. The GCM and the C²-Synthia module were suitable for estimating δ values and screening excipients that are similar in structure (e.g. tributyrin, tricaproin and tricaprolylin). The δ_{HAN} was useful for screening polar excipients that have the potential to engage in hydrogen-bonding interactions with DTX such as triglycerides and vitamin E. In order to estimate the solubility of DTX in excipients based on δ values, one also needs to consider both the $\Delta\delta$ values of the DTX-excipient pairs and the structures of the compounds. The MD simulation method using CED to calculate δ_{HIL} and χ_{FH} values was the optimal *in silico* method for determining the solubility of DTX in excipients. The χ_{FH} values obtained from MD simulations were shown to be useful for obtaining an accurate estimate of the solubility of DTX in excipients. Further studies will calculate the interaction energy associated with hydrogen-bonding between DTX and excipients. Overall, the present

study demonstrated the validity of the computational model as a reliable analytical tool for designing drug formulations.

ACKNOWLEDGMENTS

The authors are grateful to Natural Sciences and Engineering Research Council (NSERC) for funding this research.

REFERENCES

1. S. W. Yi, Y.-H. Kim, I. C. Kwon, J. W. Chung, J. H. Park, Y. W. Choi, and S. Y. Jeong. Stable Lipidolized emulsions for hepatoma targeting and treatment by transarterial chemoembolization. *J. Control. Release* **50**:135–143 (1998).
2. I.-H. Lee, Y. T. Park, K. Roh, H. Chung, I. C. Kwon, and S. Y. Jeong. Stable paclitaxel formulations in oily contrast medium. *J. Control. Release* **102**:415–425 (2005).
3. R. G. Strickley. Solubilizing Excipients in Oral and Injectable Formulations. *Pharm. Res.* **21**:201–230 (2004).
4. M. N. Khalid, P. Simard, D. Hoarau, A. Dragomir, and J.-C. Leroux. Long circulating poly(ethylene glycol)-decorated lipid nanocapsules deliver docetaxel to solid tumors. *Pharm. Res.* **23**:752–758 (2006).
5. P. Kan, Z.-B. Chen, C.-J. Lee, and I.-M. Chu. Development of nonionic surfactant/phospholipid o/w emulsion as a paclitaxel delivery system. *J. Control. Release* **58**:271–278 (1999).
6. J. G. Wenzel, K. S. Balaji, K. Koushik, C. Navarre, S. H. Duran, C. H. Rahe, and U. B. Kompella. Pluronic F127 gel formulations of deslorelin and GnRH reduce drug degradation and sustain drug release and effect in cattle. *J. Control. Release* **85**:51–59 (2002).
7. C. A. Lipinski, F. Lombardo, B. W. Dominy, and P. J. Feeney. Experimental and computational approaches to estimate solubility and permeability in drug discovery and development settings. *Adv. Drug Deliv. Rev.* **23**:3–25 (1997).
8. M. E. Aulton. *Pharmaceutics: The Science of Dosage Form Design* 2nd ed.; Elsevier Science Limited: Churchill Livingstone, 2002.
9. M. Kreilgaard. Influence of microemulsions on cutaneous drug delivery. *Adv. Drug Deliv. Rev.* **54**:S77–S98 (2002).
10. N. S. Bhattachar, L. A. Deschenes, and J. A. Wesley. Solubility: it's not just for physical chemists. *Drug Discov. Today* **11**:1012–1018 (2006).
11. B. E. Eichinger, D. Rigby, and J. Stein. Cohesive properties of Ultem and related molecules from simulations. *Polymer* **43**:599–607 (2002).
12. S. S. Patnaik, and R. Pachter. A molecular simulations study of the miscibility in binary mixtures of polymers and low molecular weight molecules. *Polymer* **43**:415–424 (2002).
13. J. Ennari, L.-O. Pietilä, V. Virkkunen, and F. Sundholm. Molecular dynamics simulation of the structure of an ion-conducting PEO-based solid polymer electrolyte. *Polymer* **43**:5427–5438 (2002).
14. T. Li, D. O. Kildsig, and K. Park. Computer simulation of molecular diffusion in amorphous polymers. *J. Control. Release* **48**:57–66 (1997).
15. J. H. Poupaert, and P. Couvreur. A computationally derived structural model of doxorubicin interacting with oligomeric polyalkylcyanoacrylate in nanoparticles. *J. Control. Release* **92**:19–26 (2003).
16. T. Spyriouni, and C. Vergelati. A molecular modeling study of binary blend compatibility of polyamide 6 and poly(vinyl acetate) with different degrees of hydrolysis: an atomistic and mesoscopic approach. *Macromolecules* **34**:5306–5316 (2001).
17. M. Zhang, P. Choi, and U. Sundararaj. Molecular dynamics and thermal analysis study of anomalous thermodynamic behavior of poly(etherimide)/polycarbonate blends. *Polymer* **44**:1979–1986 (2003).
18. S. H. Jacobson. Molecular modeling studies of polymeric transdermal adhesives: structure and transport mechanisms. *Pharmaceutical Technology* **23**:122–130 (1999).

19. Y.-M. Lam, G. Goldbeck-Wood, and C. Boothroyd. Mesoscale Simulation and cryo-TEM of Nanoscale Drug Delivery Systems. *Molecular Simulation* **30**:239–247 (2004).
20. G. Srinivas, D. E. Discher, and M. L. Klein. Self-assembly and properties of diblock copolymers by coarse grain molecular dynamics. *Nature Materials* **3**:638–644 (2004).
21. G. Srinivas, and M. L. Klein. Coarse-grain molecular dynamics simulations of diblock copolymer surfactants interacting with a lipid bilayer. *Molec. Phys.* **102**:883–889 (2004).
22. D. Pavel, and J. Lagowski. Computationally designed monomers and polymers for molecular imprinting of theophylline and its derivatives. *Polymer* **46**:7528–7542 (2005).
23. O. Pradier, M. Rave-Fränk, J. Lehmann, E. Lücke, O. Boghun, C.-F. Hess, and H. Schmidberger. Effects of docetaxel in combination with radiation on human head and neck cancer cells (ZMK-1) and cervical squamous cell carcinoma cells (CASKI). *Int. J. Cancer* **91**:840–845 (2001).
24. J. E. Cortes, and R. Pazdur. Docetaxel. *J. Clin. Oncol.* **13**:2643–2655 (1995).
25. E. K. Rowinsky, and R. C. Donehower. Drug therapy: paclitaxel (Taxol). *N. Engl. J. Med.* **332**:1004–1014 (1995).
26. U.S. Food and Drug Administration, date of access: May 2007, <http://www.fda.gov/bbs/topics/news/2004/NEW01068.html>.
27. U.S. Food and Drug Administration, date of access: May 2007, <http://www.fda.gov/bbs/topics/NEWS/2006/NEW01493.html>.
28. U.S. Food and Drug Administration, date of access: May 2007, <http://www.fda.gov/bbs/topics/ANSWERS/2001/ANS01101.html>.
29. U.S. Food and Drug Administration, date of access: May 2007, <http://www.fda.gov/cder/rdm/internetftp.htm>.
30. U.S. Food and Drug Administration, date of access: May 2007, <http://www.cancer.gov/cancertopics/druginfo/fda-docetaxel>.
31. J. H. Hildebrand, and R. L. Scott. *The Solubility of Non-electrolytes*, 3rd ed., Reinhold Publishing Corporation, New York, 1950.
32. W. Blokzijl, and J. B. F. N. Engberts. Hydrophobic effects. Opinions and facts. *Angew. Chem. Int. Ed. Engl.* **32**:1545–1579 (1993).
33. M. H. Abraham. Scales of solute hydrogen-bonding: their construction and application to physicochemical and biochemical processes. *Chem. Soc. Rev.* **22**:73–83 (1993).
34. R. F. Fedors. A method for estimating both the solubility parameters and molar volumes of liquids. *Polym. Eng. Sci.* **14**:147–154 (1974).
35. E. Ruckenstein, and I. Shulgin. Solubility of drugs in aqueous solutions. Part 1. Ideal mixed solvent approximation. *Int. J. Pharm.* **258**:193–201 (2003).
36. Accelrys Software Inc., Cerius2 Simulation & Prediction, Release 4.6, San Diego: Accelrys Software Inc., 2001.
37. T. Higuchi, and K. A. Connors. Phase-solubility techniques. *Advan. Anal. Chem. Instr.* **4**:117–212 (1965).
38. H. van der Waterbeemd, H. Lennernäs, P. Artursson. *Drug Bioavailability: Estimation of Solubility, Permeability, Absorption and Bioavailability*. Wiley VCH Verlag GmbH & Co. KGaA, Weinheim, 2003, Chapters 1 and 6.
39. M. M. A. Omari, M. B. Zughul, J. E. D. Davies, and A. A. Badwan. Thermodynamic enthalpy–entropy compensation effects observed in the complexation of basic drug substrates with β -cyclodextrin. *J. Incl. Phenom. Macrocycl. Chem.* **57**:379–384 (2007).
40. K. G. H. Desain, and H. J. Park. Solubility studies on valdecoxib in the presence of carriers, cosolvents, and surfactants. *Drug Dev. Res.* **62**:41–48 (2004).
41. R. Singh, M. Ajagbe, S. Bhamidipati, Z. Ahmad, and I. Ahmad. A rapid isocratic high-performance liquid chromatography method for determination of cholesterol and 1,2-dioleoyl-sn-glycero-3-phosphocholine in liposome-based drug formulations. *J. Chromatogr. A* **1073**:347–353 (2005).
42. B. Vaisman, A. Shikanov, A. J. Domb. Normal phase high performance liquid chromatography for determination of paclitaxel incorporated in a lipophilic polymer matrix. *J. Chromatogr. A* **1064**:85–95 (2005).
43. S. K. Tahir, M. A. Nukkala, N. A. Z. Mozny, R. B. Credo, R. B. Warner, Q. Li, K. W. Woods, A. Claiborne, S. L. Gwaltney, D. J. Frost, H. L. Sham, S. H. Rosenberg, and S.-C. Ng. Biological activity of A-289099: an orally active tubulin-binding indolyloxazoline derivative. *Mol. Cancer Ther.* **2**:227–233 (2003).
44. D. W. van Krevelen. *Properties of Polymers*. 3rd ed.; Elsevier Scientific Pub. Co.: New York, 1990.
45. M. Waldman, and A. T. Hagler. New combining rules for rare gas van der Waals parameters. *J. Comput. Chem.* **14**:1077–1084 (1993).
46. P. Gestoso, and J. Brisson. Towards the simulation of poly(vinyl phenol)/poly(vinyl methyl ether) blends by atomistic molecular modelling. *Polymer* **44**:2321–2329 (2003).
47. J. A. Mason, and L. H. Sperling. *Polymer Blends and Composites*; Plenum Press: New York, 1976.
48. J. A. McCammon. *Dynamics of Proteins and Nucleic Acids*; Press Syndicated of the University of Cambridge: New York, 1989; pp. 60–65.
49. M. P. Allen, and D. J. Tildesley. *Computer Simulation of Liquids*; Clarendon Press Oxford, 1987.
50. H. Sun. COMPASS: An ab Initio Force Field optimized for condensed-phase applications-overview with details on alkane and benzene compounds. *J. Phys. Chem. B* **102**:7338–7364 (1998).
51. D. Rigby, H. Sun, and B. E. Eichinger. Computer simulations of poly(ethylene oxide): force field, PVT diagram and cyclization behavior. *Polym. Inter.* **44**:311–330 (1997).
52. M. J. Hwang, T. P. Stockfisch, and A. T. Hagler. Derivation of class II force fields. 2. Derivation and characterization of a class II force field, CFF93, for the alkyl functional group and alkane molecules. *J. Am. Chem. Soc.* **116**:2515–2525 (1994).
53. J. M. G. Cowie. *Polymers: Chemistry and Physics of Modern Materials*, 2nd ed.; Nelson Thornes Ltd.: Cheltenham, 1991, Chapter 8.
54. C. F. Fan, B. D. Olafson, and M. Blanco. Application of molecular simulation to derive phase diagrams of binary mixtures. *Macromolecules* **25**:3667–3676 (1992).
55. F. H. Case, and J. D. Honeycutt. Will my polymers mix? - Applications for modeling to study miscibility, compatibility and formulation. *TRIP* **2**:256 (1994).
56. P. J. Flory. *Principles of Polymer Chemistry*; Cornell University Press: Ithaca, New York, 1953.
57. D. Merino-Garcia, and S. Corraera. A shortcut application of a Flory-like model to asphaltene precipitation. *J. Dispersion Sci. Technol.* **28**:339–347 (2007).
58. P. Bahadur, and N. V. Sastry. *Principles of Polymer Science*, 2nd ed.; Alpha Science International Ltd.: Oxford, UK, 2005, Chapter 8.
59. H. Elbs, and G. Krausch. Ellipsometric determination of Flory-Huggins interaction parameters in solution. *Polymer* **45**:7935–7942 (2004).
60. *Polymer Data Handbook*, Oxford University Press, Inc., 1999.
61. M. R. Paillasse, C. Deraeve, P. de Medina, L. Mhamdi, G. Favre, M. Poirot, S. Silvente-Poirot. Insights into the cholecystokinin 2 receptor binding site and processes of activation. *Mol. Pharmacol.* **70**:1935–1945 (2006).
62. S. Nosé. Constant temperature molecular dynamics methods. *Prog. Theoret. Phys. Supplement* **103**:1–46 (1991).
63. S. Nosé. A molecular dynamics method for simulations in the canonical ensemble. *Molec. Phys.* **52**:255–268 (1984).
64. D. Orloff, date of access: May 2007, <http://www.fda.gov/cder/foi/label/2002/18920s024lbl.pdf>.
65. U.S. Food and Drug Administration, date of access: May 2007, http://www.fda.gov/cder/foi/label/2004/21671_depoDur_lbl.pdf.
66. U.S. Food and Drug Administration, date of access: May 2007, <http://www.fda.gov/cder/da/da0900.htm>.
67. U.S. Food and Drug Administration, date of access: May 2007, <http://www.accessdata.fda.gov/scripts/cdrh/cfdocs/cfcfr/CFRSearch.cfm?fr=172.515>.
68. U.S. Food and Drug Administration, date of access: May 2007, <http://www.accessdata.fda.gov/scripts/cdrh/cfdocs/cfcfr/CFRSearch.cfm?fr=184.1903>.
69. U.S. Food and Drug Administration, date of access: May 2007, <http://www.fda.gov/cder/da/ddpa296.htm>.
70. D. Mastropaolo, A. Camerman, Y. Lou, G. D. Brayer, and N. Camerman. Crystal and molecular structure of paclitaxel (Taxol). *Proc. Natl. Acad. Sci.* **92**:6920–6924 (1995).
71. R. T. Liggins, W. L. Hunter, and H. M. Burt. Solid-state characterization of paclitaxel. *J. Pharm. Sci.* **86**:1458–1463 (1997).

72. L. Zhao, and S.-S. Feng. Effects of lipid chain length on molecular interactions between paclitaxel and phospholipid within model biomembranes. *J. Colloid Interface Sci.* **274**:55–68 (2004).
73. J. H. Yin, Y. Noda, N. Hazemoto, and T. Yotsuyanagi. Distribution of protease inhibitors in lipid emulsions: gabexate mesilate and camostat mesilate. *Chem. Pharm. Bull.* **53**:893–898 (2005).
74. D. J. Greenhalgh, A. C. Williams, P. Timmins, and P. York. Solubility parameters as predictor of miscibility in solid dispersions. *J. Pharm. Sci.* **88**:1182–1190 (1999).
75. T. V. M. Sreekanth, and K. S. Reddy. Analysis of solvent-solvent interactions in mixed isosteric solvents by inverse gas chromatography. *Chromatographia* **65**:325–330 (2007).
76. J. de Wit, G. A. van Ekenstein, and G. ten Brinke. Interaction between poly(vinyl pyridine) and poly(2,6-dimethyl-1,4-phenylene oxide): A copolymer blend miscibility study. *Polymer* **48**:1606–1611 (2007).
77. G. O. R. A. van Ekenstein, R. Meyboom, and G. ten Brinke. Determination of the Flory-Huggins interaction parameter of styrene and 4-vinylpyridine using copolymer blends of poly(styrene-co-4-vinylpyridine) and polystyrene. *Macromolecules* **33**:3752–3756 (2000).
78. S. M. Ali, M. Z. Hoemann, J. Aubé, L. A. Mitscher, G. I. Georg, R. McCall, and L. R. Jayasinghe. Novel cytotoxic 3'-(tert-butyl) 3'-dephenyl analogs of paclitaxel and docetaxel. *J. Med. Chem.* **38**:3821–3828 (1995).